J. Physiol. (1984), **352**, *pp.* 739–757
With 6 text-figures
Printed in Great Britain

CABLE ANALYSIS IN QUIESCENT AND ACTIVE SHEEP PURKINJE FIBRES

BY MILTON L. PRESSLER

*From the Department of Physiology, University of Berne, CH-3012 Berne, Switzerland and the Krannert Institute of Cardiology, Department of Medicine, Indiana University School of Medicine, Indianapolis, IN 46202, U.S.A.**

(*Received 24 January 1984*)

SUMMARY

1. Cable properties of sheep cardiac Purkinje fibres were studied under resting and paced conditions. Standard micro-electrode techniques were used to apply intracellular current pulses and record the resultant voltage changes at various distances from the current input. In a parallel set of experiments, fibre dimensions were measured after freezing and serial sectioning.

2. Fibres selected on the basis of a cylindrical appearance had approximately uniform cross-sectional diameters which varied $\pm 12\%$ along their length.

3. Electrotonic potentials recorded at rest and in diastole (under conditions that minimized diastolic depolarization) adhered quite closely to the behaviour expected for a unidimensional cable provided voltages were recorded $\geqq$ one fibre diameter from the current source.

4. The unidimensional space constant, input resistance, and membrane time constant were significantly larger during quiescence than in diastole. These differences were accounted for by a 90% increase in membrane resistance at rest. There was no significant change in internal longitudinal resistance nor membrane capacitance associated with activity.

5. The voltage distribution close to the current input (i.e. within one fibre diameter) strongly deviated from the theoretical three-dimensional voltage decay expected for a homogeneous cylinder. This finding suggests that the transverse resistance to current flow is much greater than the longitudinal resistance.

6. The anisotropic behaviour within the cardiac Purkinje fibre may explain several previous observations: (i) the lack of a relationship between conduction velocity and fibre diameter; and (ii) the much shorter liminal length for excitation in Purkinje fibres than for point-stimulated squid axons.

INTRODUCTION

Studies of the passive electrical properties of cardiac tissue usually have been performed on quiescent preparations (e.g. Fozzard, 1966; Weidmann, 1970; Schoenberg, Dominguez & Fozzard, 1975). In addition, quiescent preparations often have been

* Present address.

used in studies of intracellular ionic activities due to less 'technical' difficulties associated with non-beating strands. Inferences from the results of these studies have been extended to the behaviour of the beating heart on the assumption that the cellular response is equivalent. However, the extrapolation of resting studies to actively beating hearts may not be justifiable especially considering the changes in internal longitudinal resistance (Bredikis, Bukauskas & Veteikis, 1981), outward membrane current (Cohen, Falk & Kline, 1981), intracellular sodium activity (Cohen, Fozzard & Sheu, 1982) and intracellular calcium activity (Lado, Sheu & Fozzard, 1982) observed during stimulation.

Unfortunately, measurements of changes in passive electrical properties during cellular activity have several theoretical limitations. Several investigators (Lieberman, Sawanobori, Kootsey & Johnson, 1975; Sachs, 1976; Kootsey, Johnson & Lieberman, 1977) have discussed the problems of longitudinal and time-dependent voltage gradients that limit the applicability of unidimensional cable theory to spontaneously depolarizing cells. Furthermore, there is uncertainty as to how well a multicellular structure of complex anatomy conforms to the ideal unidimensional cable model. Therefore, it seemed warranted to re-examine the applicability of cable theory to active and resting sheep cardiac Purkinje fibres. This seemed especially cogent in view of recent findings that the direction and magnitude of CO_2-related changes in internal longitudinal resistance may depend upon whether the preparation is resting or active (M. L. Pressler, unpublished observations). The possibility of three-dimensional voltage decay near the current-injecting electrode tip was explored and the longitudinal uniformity of fibre diameter measured from serial sections of several preparations. The results suggest that the resting and active sheep Purkinje fibre adheres to the behaviour of a unidimensional cable under conditions that minimize diastolic depolarization. Significant deviations from the theory occur within one fibre diameter of the current-electrode tip where the observed voltage changes are much greater than predicted.

METHODS

General. Sheep hearts were obtained from a local slaughter-house and transported to the laboratory in chilled, Heparin-containing Tyrode solution. Thin, externally unbranched Purkinje preparations ($\sim$ 400 μm outer diameter; $\sim$ 7 mm in length) were cut free from the endocardium and placed in oxygenated Tyrode solution at room temperature. Preparations without visible internal branches were transferred to a tissue bath (volume $\sim$ 1·6–1·7 ml) and superfused with Tyrode solution (2–3 ml/min) of the following composition (mmol/l): NaCl, 123; KCl, 5·4; $NaHCO_3$, 21·4; NaH_2PO_4, 0·65; $CaCl_2$, 2·0; $MgCl_2$, 0·5; glucose, 5·5. The Tyrode solution was aerated with 95 % O_2–5 % CO_2 (pH 7·36 $\pm$ 0·01) and warmed to 36 $\pm$ 1 °C. Preparations were held at slack length by a tiny piece of nylon stocking which was pinned to a layer of Sylgard (Dow-Corning, Seneffe, Belgium). Brief stimuli (2 ms duration, 1·5–2 times threshold) were applied to the end of the preparation through a coaxial needle electrode. Stimulated preparations were paced at 2 Hz, a value close to the mean intrinsic heart rate of sheep (Boyett & Jewell, 1980). A recovery period of at least one hour elapsed before any experimental interventions.

Recording techniques. After the recovery period, action potentials were recorded at several locations (three to five) to assess the functional homogeneity of the preparation along its length. Preparations were considered acceptable if there was $\leqq$ 5 mV difference in transmembrane potential (V_m), a mean value for V_m of at least -80 mV and $\leqq$ 20 ms difference in action potential duration among the recording sites. Cable analysis was performed using a multiple micro-electrode technique (for details of the conventional techniques and other methodological details see Pressler,

Elharrar & Bailey, 1982). One micro-electrode used for current injection (filled with either 3 M-KCl or 2·5 M-K citrate, d.c. tip resistance 12–22 MΩ) was impaled as close as possible to one end of the fibre (mean distance from cut end ~ 100 μm). Assessment of the exact placement of the current electrode from the end of the cell column was hampered by slight retraction of the fibre within its connective tissue sheath. Recording micro-electrodes were filled with 3 M-KCl (d.c. tip resistance 12–16 MΩ). In most experiments, the position of the two recording electrodes was maintained at a constant distance from the current-injecting electrode (approximately 350 and 1400 μm). However, in some experiments, the recording electrodes were moved along the length of the fibre so that recordings could be obtained from additional sites. Experiments were considered acceptable for analysis when the current-injecting electrode remained intracellular throughout the entire period of experimental studies (lasting 3–6 h). This helped to insure a stable relationship between the tip of the current-injecting micro-electrode and the conductive core of cells.

A common bath reference (Ag/AgCl pellet) was used for all electrodes. Recording and current-passing electrodes were connected via Ag/AgCl holders to the input stage of high-impedance, unity-gain electrometers (respectively WPI M750 and WPI M707, WP Instruments, New Haven, CT, U.S.A.). Small hyperpolarizing current pulses (intensity 50 ± 20 nA (S.D.), duration 120–300 ms) were applied intracellularly at 7 s intervals. During pacing, current pulses were applied in diastole at the middle of a 1 s pause in stimulation. Three to eight electrotonic potentials were obtained at every recording location under each set of experimental conditions and the results averaged. The duration of the current pulse was adjusted so that the electrotonic potential amplitude reached steady-state. Action potentials, electrotonic potentials and the voltage output of the current-passing amplifier circuit (which was proportional to the current intensity) were displayed on an oscilloscope and photographs taken of the oscilloscopic traces. Measurements of action potential characteristics, steady-state amplitude of the electrotonic potentials (ΔV), the time to reach 50 % of ΔV ($t_{\frac{1}{2}}$), and current intensity (I_0) were performed from projector enlargements of the developed film. Noise on the amplified potential records was $\leqq 0{\cdot}4$ mV peak-to-peak. Stereoscopic measurements of inter-electrode distance and preparation geometry were made with a calibrated micrometre eye-piece at 40 × magnification.

Analysis of electrotonic potentials. Analysis of the data followed classical cable theory (Hodgkin & Rushton, 1946; Weidmann, 1952; Jack, Noble & Tsien, 1975). For long preparations ($> 3\lambda$ in length (L), denoted 'infinite case'), the space constant (λ) and membrane time constant (τ_m) were derived from linear regression analysis of ln (ΔV) *versus* inter-electrode distance (x) (slope $-1/\lambda$) and $t_{\frac{1}{2}}$ *versus* x (slope $\tau_m/2\lambda$) respectively. The voltage deflexion at the current input (V_0) was obtained by extrapolating the semilogarithmic plot to the point of current input ($x = 0$). The input resistance (R_{in}) was calculated as $R_{in} = V_0/I_0$. For shorter preparations ($L < 3\lambda$), equations for a cable terminated by an infinite resistance at $x = L$ (Weidmann, 1952) were employed to determine λ and R_{in} from the experimental data. An initial estimate of λ and V_0 was obtained from the infinite case equations. Subsequently, linear regression analysis was performed of $\text{arcosh}\,[(\Delta V/V_0)\cosh(L/\lambda)]$ *versus* $(L-x)$ to determine a new value of λ (slope of this relation $= 1/\lambda$). The new value of λ then was used to recalculate V_0 via the following equation: $V_0 = \{\Delta V \cosh(L/\lambda)\}/\{\cosh[(L-x)/\lambda]\}$. The values of λ and V_0 obtained by this method were reinserted into the above equations and the process repeated until the difference in λ and V_0 from the preceding values was $< 0{\cdot}1$ % (five to ten iterations). Correlation coefficients were determined from the linear regression analysis using experiments with multiple (> 2) recordings sites. This was done to assess the degree of agreement between the measurements and the linear relationships predicted for a unidimensional cable.

The intrinsic electrical constants, internal longitudinal resistance per unit length (r_i), membrane resistance times unit length (r_m), and membrane capacitance per unit length (c_m), were derived from the values of λ, τ_m and R_{in} using the following equations:

'infinite case':

$$r_i = R_{in}/\lambda,\ r_m = r_i\lambda^2,\ c_m = \tau_m/r_m;$$

cable terminated by infinite resistance:

$$r_i = R_{in}/[\lambda \coth(L/\lambda)],\ r_m = r_i\lambda^2,\ c_m = \tau_m/r_m.$$

The extrinsic or specific electrical constants were obtained from the following equations assuming a cylindrical geometry for the Purkinje fibre: $R_i = \pi a^2 r_i,\ R_m = 2\pi a r_m,\ C_m = c_m/2\pi a$, where

a = mean radius of the fibre. Extracellular resistance was neglected since the preparation was immersed in a large volume of conductive solution.

Dimensional analysis. Dimensional measurements were performed in concert with the electrical measurements. The terms used to describe various anatomical structures will be defined to avoid semantic confusion regarding their use in this paper. The word 'fibre' has been employed to mean the cluster of cells bounded by a dense connective tissue sheath which forms the conductive core of the over-all structure. The word 'preparation' has been chosen to designate the entire structure dissected from the sheep ventricle within which one or more fibres are contained. 'Outer diameter' refers to a dimension of the entire preparation. The over-all length, outer diameter and apparent fibre diameter (i.e. the diameter of a translucent structure within the preparation) were measured in all preparations using the calibrated ocular graticule of a stereomicroscope. In some of the preparations, further dimensional analysis was performed. Subsequent to cable analysis, the preparation was immersed for 30–60 s in isopentane pre-cooled in liquid N_2. Then the preparation was stored in liquid N_2 until sectioning. The preparations were aligned perpendicular to their long axis in a cryomicrotome (Leitz 1720, Wetzlar, F.R.G.) and 10 μm serial sections made at -14 °C over 1–3 mm. The resultant sections were air dried, stained with 1 % Toluidine Blue and examined at 100 × and 320 × magnifications with an inverted phase-contrast microscope (Leitz Diavert, Wetzlar, F.R.G.). The short and long axes of the outer preparation diameter and the fibre diameter were measured directly using a calibrated eye-piece graticule (1 unit = 12·4 μm at 100 ×, 3·84 μm at 320 ×). Every fourth or fifth section was measured and grossly distorted or folded sections rejected. An equivalent circular diameter was computed from the measured long and short axes by approximating the cross-section as elliptical. The resultant outer diameters were compared to those measured in the stereomicroscope before sectioning (when the preparations were alive in the tissue bath). There was no statistically significant difference between the mean $\pm$S.E. of mean outer diameter measured stereomicroscopically (462 ± 32 μm) and the mean $\pm$S.E. of mean equivalent diameter from the thick sections (454 ± 20 μm). The cross-sectional measurements were examined for deviations from a true perpendicular cut by the following criteria. Each equivalent outer diameter was compared to the stereomicroscopic outer diameter with a tolerance limit of ± 50 μm (which was approximately the variation of the outer diameter along the length of the preparation). Those sections having outer diameters outside of this tolerance limit were considered 'oblique' or 'shrunken' and not included within the mean equivalent fibre diameter that was derived. This selection process lowered the estimate of the fibre diameter by ~ 6 % and perhaps corrected for some of the deficiencies of the method.

Statistics. Statistical analysis was performed using Student's t test for paired data (Snedecor & Cochran, 1967). The difference between mean values was considered to be statistically significant for $P < 0{\cdot}05$.

RESULTS

Purkinje fibre geometry and dimensions

One limitation for the application of cable theory to biological preparations is the need to assume an ideal geometry. The usual simplification for cardiac Purkinje fibres is that the structure can be approximated by a right circular cylinder having a core of uniform resistivity per unit length. To test the deviation from the ideal, several experiments were performed to measure the variation of the fibre diameter along the length of the preparation. Preservation, staining and sectioning techniques were designed to preserve geometrical parameters and not to enhance fine anatomical details. Hence, no attempt was made to study the well-known light microscopic appearance of sheep Purkinje fibres. Instead, measurements were made of transverse dimensions of preparations viewed through the stereomicroscope and compared to those obtained after freezing (in liquid N_2-cooled isopentane) and serial sectioning.

Preparations were selected for cable analysis on the basis of no visible external or internal branches, large, superficial and apparently single fibres, thin over-all

TABLE 1. Comparative dimensional measurements on fibres

Fibre no.	Stereomicroscopic		Light microscopic	
	Preparation diameter (μm)	Fibre diameter (μm)	Mean $\pm$S.D. preparation diameter (μm)	Mean $\pm$S.D. fibre diameter (μm)
29.11.82	370	185	389$\pm$14	183$\pm$18
06.12.82	568	210	538$\pm$23	146$\pm$11
13.12.82	457	222	445$\pm$15	188$\pm$21
20.12.82	470	222	453$\pm$28	152$\pm$33
27.12.82	445	222	426$\pm$21	161$\pm$16
Mean	462	212	450	166*
$\pm$S.D.	$\pm$71	$\pm$16	$\pm$55	$\pm$19

Stereomicroscopic measurements were performed on living preparations in the tissue bath; light microscopic data were obtained from measurements on serial sections of the same preparations; *$P < 0.025$ compared to stereomicroscopic measurements.

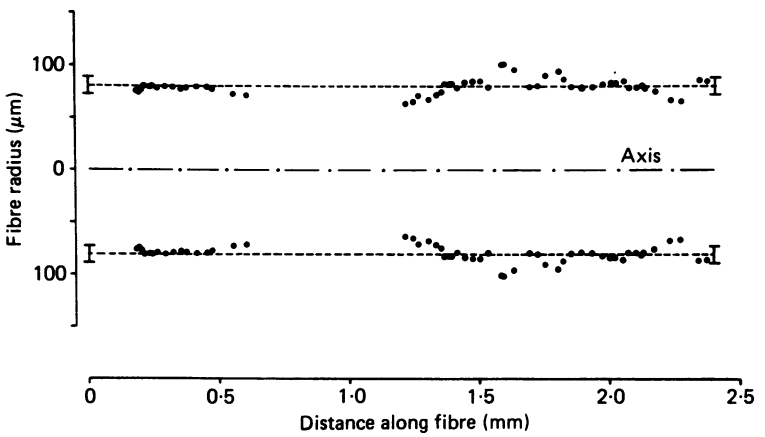

Fig. 1. Longitudinal variation of equivalent circular diameter in a serially sectioned sheep Purkinje fibre. Filled circles represent individual measurements at approximately 30–50 μm intervals; dashed line and horizontal bars denote mean $\pm$S.D. fibre radius (80·4$\pm$7·9 μm). The missing values between 0·6 and 1·2 mm arose from distortion and deterioration of one set of serial sections. Fibre no. 27.12.82.

dimensions, and minimal variation in fibre diameter. Following cable analysis, stereomicroscopic measurements were made on all preparations. In five instances, more detailed dimensional studies (i.e. freezing and serial sectioning) were performed after the physiological experiments. The sectioned preparations were found in each case to contain a large, well-circumscribed bundle of cells a few micrometres ($\sim$ 10–15 μm) from the external surface. The approximate cross-sectional appearances were elliptical in shape for both the outer preparation and fibre outlines. Short and long axes of the elliptical structures were measured at various intervals (see Methods) and an equivalent circular diameter calculated. The resultant dimensions are listed in Table 1 and an example of the variation in fibre diameter with distance is shown in Fig. 1. The fibre diameter for the series of five preparations deviated from uniformity by 7·5–21·7% (% deviation = (S.D./mean) $\times$ 100%). The mean $\pm$S.D.

deviation was 12·0 ± 5·6 %. Part of this deviation arose from imperfections in the sectioning technique and thus the figure of 12 % should be considered as an upper bound. Branching also contributed to the variation in one of the five superficial fibres. However, the branch in this case was small in size (~ 11 % of the cross-sectional area of the larger fibre) and repeatedly joined and separated from the main fibre. There was no strong evidence abrogating the geometrical assumptions made in cable theory from the branching or variation in fibre diameter that were observed.

There were a few additional findings noted in the preparations selected for cable analysis. Three of the five preparations contained additional fibres despite the external appearance of a single circumscribed structure. In two of these instances, the additional fibre was rudimentary. These fibres were much smaller in cross-sectional area (~ 10–15 % of the large superficial fibre), lay deep within the preparation and tapered to vanishingly small dimensions ($\leqq 20\ \mu$m diameter) in several regions. However, a significant additional fibre was observed deep within the largest preparation. This fibre divided into two smaller fibres which branched and rejoined at several intervals. Careful inspection of more than 100 sections showed no connexion of the deeper fibre(s) with the superficial fibre. On this basis, the superficial fibres were considered to be isolated and their dimensions (see Table 1) used to derive the specific electrical constants.

Comparison between measurements obtained via the stereomicroscope and from light microscopic examination of serial sections revealed no significant difference in over-all diameter. In contrast, there was a 28 % larger fibre diameter ($P < 0{\cdot}025$) measured using the stereomicroscope. The evidence suggests that the preservation technique did not impart any substantial expansion or contraction artifact to the fibre dimensions in the serial sections since the over-all diameters were roughly equal (± 2 %). Instead, it is thought that the measurements from the frozen sections were more reliable because the entire outline of the fibre could be visualized directly during the measurement. The factors which limited the accuracy of the stereomicroscopic measurements included: (1) problems with angular orientation of the fibre with regard to the one dimension visible to an external observer; (2) positioning of additional fibres beneath the most superficial one so that the outline appeared larger from superposition; (3) difficulties in discriminating borders through the overlying connective tissue (enhancing observer bias); (4) parallax from the distant vantage point. The net result was that the inherent problems with the stereomicroscopic assessment of internal dimensions outweighed the potential artifacts of fibre preservation and sectioning.

Adherence of resting and paced Purkinje fibres to cable theory

Valid application of cable theory to electrotonic potentials measured in Purkinje fibres is predicated not only upon geometrical simplicity but also upon constancy of electrical properties in space and time. During diastolic depolarization, the variation of membrane potential and resistance with time would seem to invalidate the application of the equations derived by Hodgkin & Rushton (1946). Lieberman *et al.* (1975) have studied this situation in some detail (in cultured chick cardiac strands) using the approximation that membrane resistance is a linear function of time. In the present studies, a different approach was utilized. Action potentials were recorded

at multiple sites along the length of the fibre to determine if longitudinal non-uniformities existed in the electrical properties (e.g. from injury during cutting or dissection). In addition, superfusate [K^+] was 5·4 mmol/l and a relatively short pacing interval was maintained in order to minimize the rate of diastolic depolarization ($\leqq$ 1–2 mV/s). Hence, membrane potential varied a very small amount ($\leqq$ 0·4 mV) over the course of a 150–300 ms current pulse. This small change in membrane potential seemed sufficiently close to the ideal at rest to warrant assessment of how well the 'classical' cable equations described the electrotonic potentials recorded in the diastolic interval.

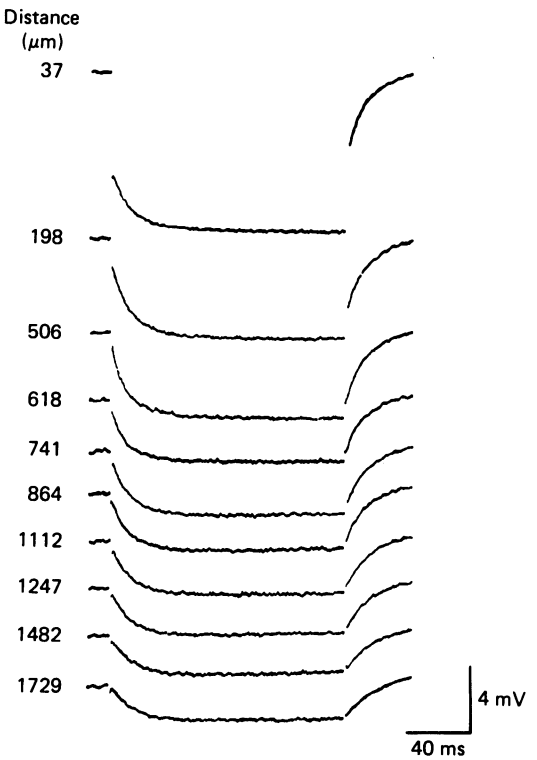

Fig. 2. Electrotonic potentials recorded at various distances from the site of current input. Sheep Purkinje fibre paced at 2 Hz with a 70 nA current pulse applied at the mid-point of a 1 s pause in pacing. Each electrotonic potential reached a steady-state value after three to five membrane time constants. Mean ±S.D. V_m was -84 ± 2 mV. Fibre no. 27.12.82.

Twelve preparations were evaluated for functional non-uniformity by recording action potentials at three or more sites along the length of the fibre (x_0 104 ± 10 μm; x_1 393 ± 35 μm; x_2 1397 ± 105 μm, where x_0 = mean ±S.E. of mean distance of the current-injecting electrode from the end of the fibre and x_1, x_2 = mean ±S.E. of mean distances of recording electrodes 1 and 2 from the current input). The transmembrane potentials (mean ±S.E. of mean) before the 'take-off' of the upstroke (V_m) were quite comparable close to the cut end and 1·4 mm distant ($V_{m,0}$, $V_{m,1}$, $V_{m,2}$ = -85 ± 1, -84 ± 1, and -84 ± 1 mV, respectively). Action potential amplitudes

(120±3, 118±2, and 122±2 mV, mean ±S.E. of mean, respectively) and action potential durations at 90% of repolarization (232±9, 233±8, and 229±8 ms, mean ±S.E. of mean, respectively) also were very similar at the various sites. There was little reason to suspect longitudinal non-uniformity in the fibres with so little spatial variation in electrical characteristics.

Fig. 2 shows a series of ten electrotonic potentials recorded in diastole at various distances (x) from the site of current application. Three electrodes were employed in

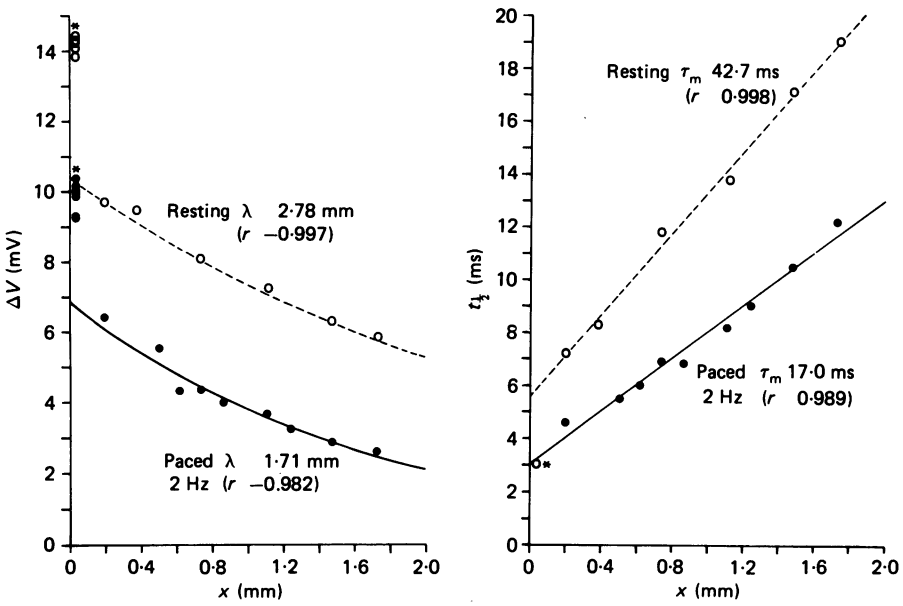

Fig. 3. Adherence of electrotonic potentials to unidimensional cable theory. Left panel: steady-state amplitude of electrotonic potentials (ΔV) *versus* distance from site of current input (x); right panel: time to reach one-half of steady-state amplitude ($t_{\frac{1}{2}}$) *versus* distance. Filled circles, electrotonic potential amplitudes recorded in diastole in a paced sheep Purkinje fibre (same experiment as Fig. 2); open circles, records after 45–95 min of quiescence. Current-injecting and one recording electrode ($x = 37$ μm) were maintained at constant sites during the entire experiment. Electrotonic potentials recorded both in diastole and at rest fitted the predictions of one-dimensional cable theory except for records close to the current input (*, excluded from analysis). Half-time measurements at $x = 37$ μm could not be obtained in the paced fibre because a transient obscured the initial time course. Space constants (λ), membrane time constants (τ_m) and correlation coefficients (r) as shown. Current intensity 70 nA. Fibre no. 27.12.82.

this experiment with two of the sites (i.e. the current-injecting and closest recording micro-electrode, $x = 37$ μm) remaining constant during the entire analysis. Each electrotonic potential reached a steady-state amplitude (ΔV) after a period of 3–5 membrane time constants. There was no evidence of 'creep' of the potential-time course provided the action potentials initially recorded were of normal amplitude and contour.

The results were analysed by fitting linear regression equations to the measurements. Fig. 3 shows a graph of the data illustrated in Fig. 2 plus additional data obtained from electrotonic potentials recorded after a 45 min period of quiescence. Except for

the measurements very close to the site of current input (marked by *), both the resting and diastolic data followed the expected behaviour of a unidimensional cable with a high degree of correlation. In four experiments performed in three paced fibres, the ΔV *versus* x relation (five to nine points in each experiment) fitted to an exponential decay ($L \geqq 3\lambda$) or a ratio of hyperbolic cosines ($L < 3\lambda$) with a mean $\pm$S.D. correlation coefficient of $-0{\cdot}990 \pm 0{\cdot}008$. In three resting fibres, the ΔV *versus* x distribution (six to seven points) fitted the exponential or hyperbolic cosine relationships with a mean $\pm$S.D. correlation coefficient of $-0{\cdot}995 \pm 0{\cdot}002$. The half-time ($t_{\frac{1}{2}}$) *versus* distance measurements fitted to a linear relation with the following mean $\pm$S.D. correlation coefficients: paced at 2 Hz, $0{\cdot}983 \pm 0{\cdot}009$; resting, $0{\cdot}997 \pm 0{\cdot}002$. The correlation for both resting and paced fibres seemed sufficiently close to the ideal to justify further interpretation of the electrotonic potentials on the basis of the Hodgkin–Rushton theory (1946).

TABLE 2. Cable properties of sheep Purkinje fibres

		Paced 2 Hz				Resting			
Fibre no.	L (mm)	V_m (mV)	λ (mm)	R_{in} (kΩ)	τ_m (ms)	V_m (mV)	λ (mm)	R_{in} (kΩ)	τ_m (ms)
22.02.82	6·67	−81	1·24	160	7·0	−79	1·90	233	18·7
05.07.82	3·78	−82	1·97	195	9·8	−76	2·36	256	13·7
16.08.82	7·27	−86	1·41	290	18·4	−75	1·86	401	33·9
23.08.82	4·76	−87	1·68	186	9·6	−77	2·46	305	18·3
18.10.82	10·3	−86	1·40	292	6·2	−80	1·84	410	13·1
25.10.82	6·57	−87	0·88	418	6·9	−75	1·16	585	16·9
01.11.82	8·08	−80	1·16	208	15·4	−76	1·34	231	26·2
08.11.82	9·19	−86	1·25	77	8·0	−71	3·36	113	48·1
27.12.82	6·15	−84	1·71	98	17·0	−72	2·78	149	42·7
Mean	6·97	−84	1·41	214	10·9	−76†	2·12*	298†	25·7*
S.E. of mean	±0·68	± 1	±0·11	±35	±1·6	± 1	±0·23	±49	±4·3

Abbreviations: L, fibre length; V_m, transmembrane potential; λ, space constant; R_{in}, input resistance; τ_m, membrane time constant; †$P < 0{\cdot}001$; *$P < 0{\cdot}01$ compared to paced values.

One-dimensional cable properties at rest and during activity

Table 2 lists the cable constants measured in nine sheep Purkinje fibres. In each experiment, the current-injecting electrode was inserted near the 'sealed' end of the fibre and remained intracellular during the entire period of quiescence and activity. Seven of the experiments were performed with a three-micro-electrode technique in which all electrodes remained constant in position during the experimental period. The last two experiments (Nos. 08.11.82 and 27.12.82) were carried out with the recording electrode location varying over six to nine positions. The recording electrode closest to the current input was placed a minimum of 150 μm (357 ± 154 μm, mean $\pm$S.D.) from the current electrode so as to avoid the complication of three-dimensional current spread in analysing the electrotonic records. Thirty to sixty minutes elapsed between measurements during diastole in paced fibres and those obtained during quiescence.

Four significant differences were apparent between resting and active fibres. The mean transmembrane potential was 8 mV less negative, the mean λ 50 % larger, mean R_{in} 39 % greater and mean τ_m 136 % greater at rest than during activity. The analysis of the changes in λ and R_{in} is shown in Fig. 4. There was no significant difference between the mean $\pm$S.E. of mean internal longitudinal resistance per unit length at rest ($1{\cdot}71 \pm 0{\cdot}47$ MΩ/cm) and during pacing ($1{\cdot}69 \pm 0{\cdot}43$ MΩ/cm). However, the mean membrane resistance times unit length nearly doubled (94 % increase) during quiescence. In addition, the effect of activity on membrane capacitance per unit length (c_m) was calculated by dividing τ_m by r_m (determined from λ and R_{in}). There was no significant difference between the mean $\pm$S.E. of mean c_m at rest and during pacing ($0{\cdot}55 \pm 0{\cdot}14$ μF/cm *versus* $0{\cdot}47 \pm 0{\cdot}10$ μF/cm).

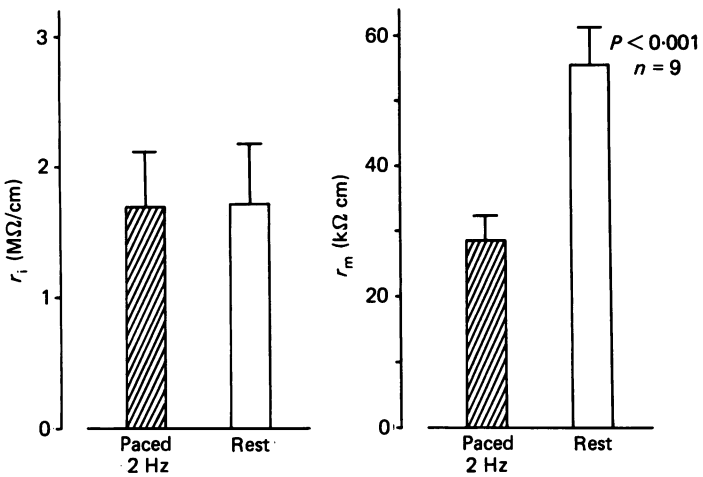

Fig. 4. Intrinsic cable constants (mean $\pm$S.E. of mean) from active and quiescent sheep Purkinje fibres. Left panel: internal longitudinal resistance per unit length (r_i); right panel: membrane resistance times unit length (r_m). Analysis of λ and R_{in} data shown in Table 2. Resting and active fibres had no significant difference in r_i but the membrane resistance was approximately twice as great at rest than in diastole.

One experiment was performed to determine the rate of change of membrane resistance with respect to the time period of quiescence. Electrotonic potentials were recorded at several minute intervals after cessation of pacing (2 Hz) and again after its resumption. Approximately 85 % of the total steady-state increase in r_m had occurred within 2–5 min of the onset of rest and 96 % of the steady-state increase after 15 min. When pacing was restored, 82 % of the total decrease in r_m had taken place after 5 min and 97 % after 10–12 min of stimulation.

Three control experiments were also undertaken to determine the changes in cable constants over time *per se* (i.e. no alterations in superfusate or pacing rate were made). During constant pacing at 2 Hz, the preparations tended to depolarize with time ($1{\cdot}1 \pm 0{\cdot}4$ mV/h, mean $\pm$S.E. of mean) and λ, R_{in} and τ_m slowly increased. The changes in r_i over time were minimal with a variation of ± 5 % around a mean decrease of 0·4 %/h. In contrast, r_m tended to increase slowly at a rate of 10 ± 5 %/h (mean

$\pm$S.E. of mean). As a consequence, 'scatter' was observed in the electrotonic potential amplitudes near the current input during cable analysis with a roving micro-electrode (see Fig. 3 and also Fig. 5*A*). The fixed recording electrode close to the current source ($x = 37$ μm) measured a progressive increase in ΔV over the time required to make more distant measurements. In this manner, the slow time-dependent changes contributed to the deviations from ideal cable behaviour and served to limit the accuracy of the roving-electrode technique.

Specific electrical constants were determined from the fibre diameters measured in the five serially sectioned preparations. Two experiments were performed at rest and five experiments during pacing (2 Hz). The mean $\pm$S.E. of mean R_i from all of these experiments was 104 ± 6 Ω cm ($n = 7$). R_m was 737 ± 112 Ω cm^2 during activity ($n = 5$) and 2920 ± 883 Ω cm^2 at rest ($n = 2$). Specific membrane capacitance (C_m) was $20{\cdot}0 \pm 1{\cdot}8$ μF/cm^2 ($n = 7$). Given the result that the surface-to-volume ratio in sheep Purkinje fibres is approximately 11·5 times that of the apparent cylindrical surface to volume ratio (Mobley & Page, 1972), the following specific constants were calulated: R_m: 8500 Ω cm^2 (paced), 33600 Ω cm^2 (resting); C_m 1·7 μF/cm^2.

Voltage gradients near the current input

The data in Fig. 3 also demonstrate that the potentials recorded near the current source deviate considerably from the predictions of one-dimensional cable equations. Three preliminary experiments (two paced, one resting) verified the finding that electrotonic potentials within 100 μm of the current input have a larger amplitude and more rapid voltage-time course than predicted from extrapolation of distant records fitted to one-dimensional cable equations. This is not surprising in that radial as well as longitudinal voltage gradients are expected to exist around a point source of current applied to a cylindrical structure (Fatt & Katz, 1953; Adrian, Costantin & Peachey, 1969; Eisenberg & Johnson, 1970). However, the inter-electrode distance must be known in terms of the radius of the conductive path in order to describe more precisely the voltage distribution near the current source.

The voltage decay in the proximity of the current electrode tip depends upon (1) the radius of the conductive path (a), and (2) the angular separation (α), depth of penetration (y), and longitudinal separation (x) of the current-injecting and recording electrode tips. The most profound three-dimensional spread ('worst case') occurs when both electrodes lie along the same longitudinal axis ($\alpha = 0°$) and both electrode tips are positioned just beneath the surface of the cylinder ($y_1 = y_2 \cong a$). Under these circumstances, the total voltage displacement as a function of distance, $V(x)$, can be described in terms of the sum of a linear one-dimensional component, $V_{1d}(x)$, and a spherical three-dimensional component, $S(x)$: $V(x) = V_{1d}(x) + 0{\cdot}5 r_i I_0 a S(x)$ (patterned after equation II.1–3, Eisenberg & Johnson, 1970). The spherical component is a complicated expression involving the summation of a series of terms in which Bessel functions of the first kind, exponential functions, and the roots of an equation containing Bessel functions are combined (for tabulation see Tables 1 and 2, Eisenberg & Johnson, 1970). The linear component depends upon the length of cable relative to the space constant (L/λ) and the position of the current-injecting electrode (i.e. near the end, mid-point, etc.). Provided the current-injecting electrode remains a finite distance from the end of the cylindrical cable (in practice x_0 is

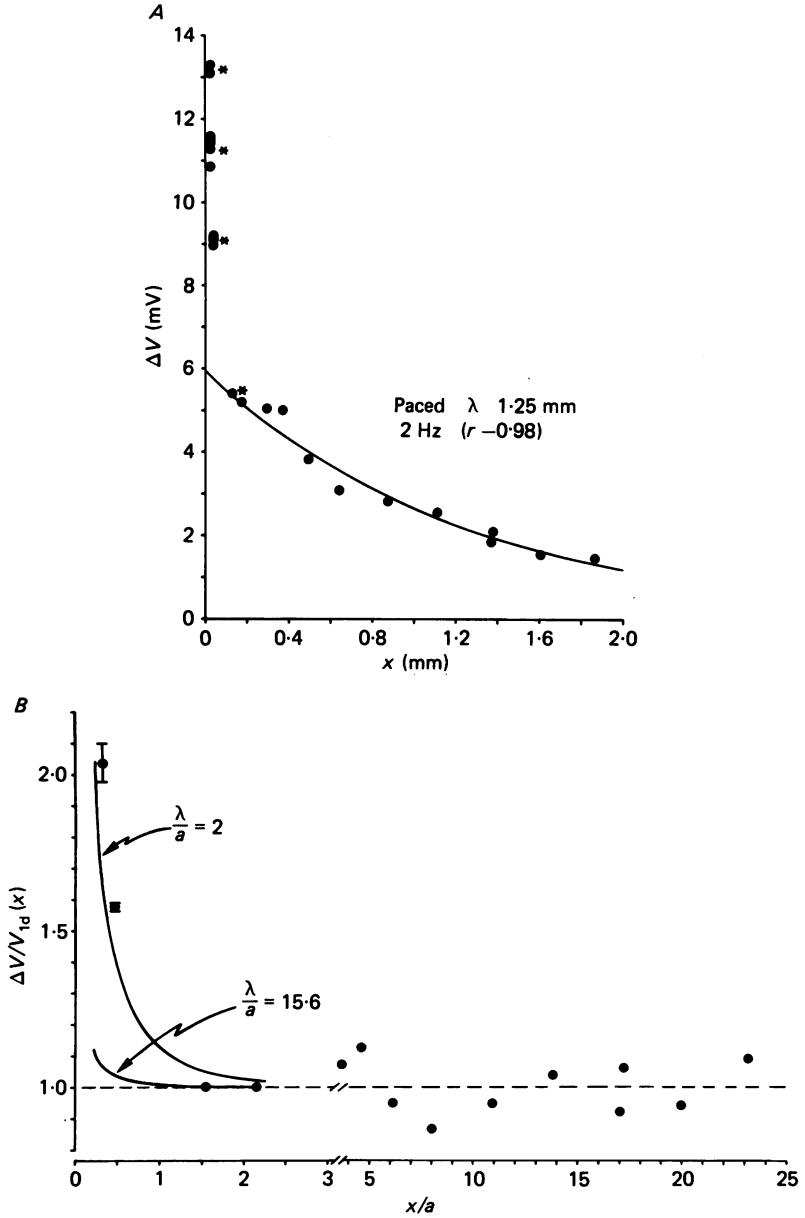

Fig. 5. Analysis of voltage decay near the current electrode tip in a paced sheep Purkinje fibre. *A*: steady-state amplitudes of electrotonic potentials (ΔV) *versus* distance from site of current injection (x). Points within one fibre diameter of the current source (marked with * at x = 25, 37, 124 and 173 μm) were excluded from analysis of the one-dimensional voltage decay (smooth curve shown: $V_{1d}(x) = V_0 \exp(-x/\lambda)$). *B*: plot of electrotonic potential amplitude (from *A*) divided by predicted one-dimensional voltage displacement ($\Delta V / V_{1d}(x)$) *versus* distance normalized by the fibre radius (x/a). Smooth curves represent the calculated three-dimensional voltage decay for two different ratios of space constant to fibre radius (λ/a). The voltage distribution near the current input followed a much steeper curve ($\lambda/a = 2$) than expected from the one-dimensional space constant/fibre radius ratio ($\lambda/a = 15{\cdot}6$). Mean $\pm$S.D. V_m was -86 ± 3 mV. Separate experiment in fibre no. 27.12.82.

almost always ≧ the radius) $V(x)$ is approximated by the following equation (for current input near the end of a semi-infinite homogeneous cylinder):

$$V(x) = I_0\sqrt{(r_m r_i)}\exp(-x/\lambda)+0{\cdot}5\, r_i I_0 a\, S(x).$$

When this relation is divided by the predicted one-dimensional voltage displacement, the expression becomes:

$$V(x)/V_{1d}(x) = \frac{2(\lambda/a)\exp(-x/\lambda)+S(x)}{2(\lambda/a)\exp(-x/\lambda)}.$$

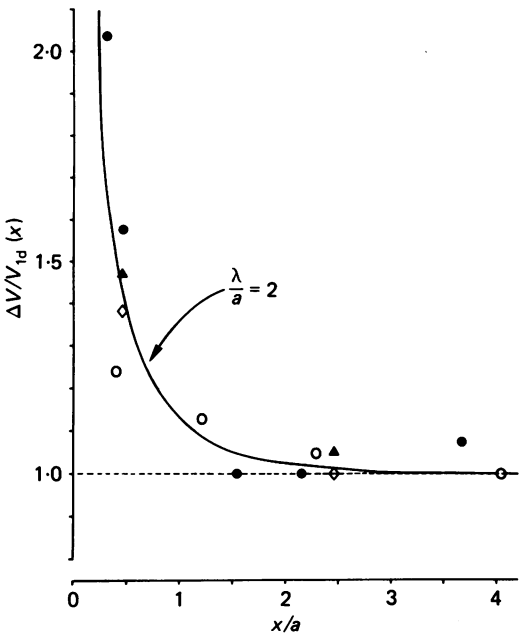

Fig. 6. Voltage distribution near current input. Combined results from four experiments in two sheep Purkinje fibres. Filled symbols represent data from paced preparations; open symbols from quiescent preparations. Smooth curve is the three-dimensional voltage decay calculated for a λ/a ratio of 2. The experimental results were described by a much steeper voltage distribution than expected from the ratio of the one-dimensional space constant to the fibre radius (λ/a: 15·6–44·0, curves not shown). Horizontal dashed line shows the result expected for an ideal one-dimensional cable. For abbreviations see Fig. 5. Fibre nos. 29.11.82 and 27.12.82.

The spatial voltage decay occurring in the vicinity of a point source of current (applied near the sealed end of a sheep Purkinje fibre) was studied in four additional experiments. In these studies, the electrical measurements were combined with the previously described anatomical measurements so that the radius of the fibre would be known. Fig. 5 illustrates one example in which the preparation was paced at 2 Hz and intracellular current applied in diastole during a 1 s interruption of the pacing train. The current-injecting micro-electrode remained intracellular throughout the experiment while two additional micro-electrodes recorded electrotonic potentials at various distances. The results (Fig. 5*A*) again demonstrated a very steep voltage decay close to the current source (points marked with a *). To evaluate the rate of

voltage decay with distance, the aforementioned three-dimensional analysis was applied to the data. Fig. 5*B* shows the steady-state voltage displacement (ΔV) divided by the expected one-dimensional voltage displacement ($V_{1d}(x)$) plotted *versus* the inter-electrode distance relative to the fibre radius (x/a). The three-dimensional voltage decay expected from the one-dimensional λ and measured radius (80 μm) lay well below the experimental points ($\lambda/a = 15{\cdot}6$). Instead, the voltage change near the current source was approximated by the smooth curve predicted for $\lambda/a = 2$. Fig. 6 combines the results from three additional experiments to those shown in Fig. 5*B*. Once again, the curvilinear relationship expected from three-dimensional cable theory (not shown) was found to rise much less steeply than the curve which best fitted the experimental results. In fact, the ratio between the λ/a fitting the experimental results ($\lambda/a \cong 2$) and the λ/a arising from potentials measured $\geqq$ one fibre diameter from the current source (λ/a 15·6–44·0) was approximately 1:10. This deviation of the results from the three-dimensional theory occurred despite fairly close adherence to the one-dimensional theory further away from the current-injecting electrode tip. In this regard, the electrotonic potential amplitudes varied a mean of $\pm 5\%$ (range 1·5–8·3 %, $n = 4$) from the amplitudes calculated from one-dimensional analysis when the recordings were made more than one fibre diameter from the current input.

DISCUSSION

Alterations in cable constants associated with activity

The alterations in cable properties shown in Table 2 may have some significance for the analysis of propagation. It is apparent that excitatory current would flow through a circuit with somewhat different characteristics than would be determined in a quiescent preparation. All of the measured constants (i.e. λ, R_{in}, τ_m) were smaller in the paced fibre than at rest. These changes appear to be due entirely to a decrease in membrane resistance with activity (see Fig. 4) and not to changes in internal longitudinal resistance or membrane capacitance. There are several possible mechanisms for the changes in r_m. Certainly, a large part of the increase in r_m at rest was related to the change in transmembrane potential. Purkinje fibres are known to hyperpolarize during rapid stimulation (Vassalle, 1970; Kline, Cohen, Falk & Kupersmith, 1980) in contrast to ventricular muscle where depolarization occurs (Kline & Morad, 1978). Hyperpolarization is associated with a rise in membrane conductance (g_m) and depolarization (up to $V_m \sim -30$ mV in Na^+-deficient solutions), a fall in g_m due to inward-going ('anomalous') rectification (Weidmann, 1955; Carmeliet, 1961; Hall, Hutter & Noble, 1963). Hellam & Studt's studies (1974) allow an estimate to be made of the voltage-dependent changes in R_m (within the -70 to -100 mV range). They measured the alterations in membrane 'slope' resistance ('R_m') at various membrane potentials (using 1–2 mm voltage-clamped sheep Purkinje fibres, $[Na^+]_o$ 137 mM, $[K^+]_o$ 5·4 mM) and derived an empirical expression for 'R_m' in terms of V_m (see their Fig. 12, Hellam & Studt, 1974). This equation predicts a 125 % increase in 'R_m' with a potential change from -84 to -76 mV. This is quite comparable to the mean increases of 94 % and 136 % that were obtained for r_m (calculated from λ and R_{in}) and τ_m, respectively, as the fibres depolarized from -84 (paced at 2 Hz) to -76 mV (resting). Unfortunately, differences in the methods

of measuring membrane resistance (i.e. d.c. membrane resistance *versus* 'slope' resistance) somewhat reduce the applicability of Hellam & Studt's equation to the present results. The concurrence of their predicted change in 'R_m' with the current findings does not exclude factors other than V_m from contributing as well. Chief amongst these would be the accumulation of K^+ and activation of the electrogenic Na^+–K^+ pump that are known to occur with stimulation of quiescent Purkinje fibres (Kline *et al.* 1980; Cohen *et al.* 1981). It is quite conceivable that pacing-related accumulation of K^+ in restricted extracellular spaces led to part of the fall in r_m that was observed. The period of time between measurements at rest and during pacing was intentionally lengthy so that these changes could reach steady state.

An additional comment is appropriate with regard to the lack of change in internal longitudinal resistance during pacing (at 2 Hz). This finding contrasts to the apparent increase in r_i found upon rapid stimulation (10–15 Hz) in rabbit atrial traebeculae (Bredikis *et al.* 1981). However, several factors complicate the interpretation of the latter results. First, measurements of input resistance in the atrial traebeculae were made using double-barrelled micro-electrodes. The absence of a potential drop across the recording barrel during current application within the extracellular space does not necessarily exclude an additional series resistance from being superimposed on the cellular input resistance when the electrode tip is intracellular (Eisenberg & Johnson, 1970). Furthermore, the determination of r_i from the measured electrotonic potentials depends upon a proper mathematical treatment of the three-dimensional current flow in an anisotropic medium. The complexity of the problem in view of the rather scanty information available about the degree of anisotropy would add considerable uncertainty to the quantitation of changes in r_i and r_m from input resistances containing a three-dimensional component. In the present study, no significant change in r_i was observed at a pacing rate of 2 Hz. This of course does not exclude the possibility that more rapid rates of stimulation might have altered the diastolic value of r_i.

Surprisingly, the amount of Ca^{2+} influx known to occur with stimulation does not seem to affect the diastolic value of r_i. This may be accounted for by several mechanisms: (1) junctional membranes may be relatively insensitive to moderate changes in free $[Ca^{2+}]_i$; (2) changes in free $[Ca^{2+}]_i$ may be confined to cellular spaces which do not (or only poorly) exchange with the perijunctional membrane space; (3) reversible changes in junctional conductance may occur that are too small or rapid to be observed with the present methods. Nevertheless, it seems reasonable from a teleological standpoint that the diastolic value of r_i might not be too different from the resting value. It would not be expected that an excitable tissue like heart would have a less conducive circuit for conduction when active than at rest.

Implications of radial voltage gradients near a point source

The striking deviation of the voltage decay near the current input from theoretical predictions (see Figs. 5 and 6) has several implications with regard to excitation and impulse propagation. The voltage distribution observed was much steeper ($\lambda/a \cong 2$) than anticipated from the measured ratio of space constant to fibre radius ($\lambda/a = 15{\cdot}6$–44). These findings are similar to an earlier result reported for dog false tendons (Pressler *et al.* 1982). This discrepancy could not be explained simply by

allowing for the inherent errors in measurement of recording and current-injecting electrode positions. Indeed, errors in longitudinal distance measurements ($\pm$10–15 μm, or $\pm$0·12–0·19 fibre radii) certainly limited the precision of the determination but this amount of lateral displacement of the data points still would not provide a reasonable fit to the predicted curve (see Fig. 5*B*). Furthermore, errors in the angle of electrode inclination (α) or depth of penetration (y) would have decreased the deviation (not enhanced it) since only the most profound theoretical case was considered (i.e. $\alpha = 0°$; $y = a$). Instead, the data suggest that the $\sim$ 10-fold greater steepness ($\lambda/a \cong 2$ *versus* $\lambda/a \cong 20$–30) of the voltage decay near the current input resulted from either: (1) constriction of the radius of the conductive path to a value much smaller than the fibre radius; and/or (2) decrease of the effective space constant to a value much smaller than apparent from the voltage decay observed further away from the current source. Such a decrease in space constant for radial *versus* longitudinal current flows (ignoring possible extracellular resistance effects) could arise either from a decrease in membrane resistance or an increase in internal resistance in the immediate vicinity of the electrode tip. The latter possibility seems to be much more likely since the transmembrane action potentials and electrotonic potentials recorded near the current source (e.g. $x = 37$ μm, Fig. 2) give no reason to suspect a lowered or changing membrane resistance. In addition, anatomical considerations suggest a simple explanation for the existence of an increased internal resistance to the radial flow of current. Several cell boundaries must be traversed for current to fill the entire fibre diameter and hence might provide additional internal impedance to current flow before it becomes essentially longitudinal. In fact, this circumstance is qualitatively the same as constricting the effective radius of the conductive path (e.g. to only the most superficial cells of the fibre). Therefore, both of the aforementioned explanations (i.e. decreased radius and/or decreased λ near the current input) actually describe the same physical situation, namely that the resistance to current flow within the Purkinje fibre is greater transversely than longitudinally. Hence, the existence of anisotropy may explain the deviation between measured and theoretical three-dimensional voltage decays near the point source of current.

The presence of anisotropy (similar to that thought to exist in ventricular muscle, e.g. Clerc, 1976; Spach, Kootsey & Sloan, 1982) would explain several puzzling observations in cardiac Purkinje fibres. The first involves the relationship between conduction velocity (θ) and fibre diameter (d). Hodgkin (1954) has described the theoretical prediction that θ for a uniform fibre immersed in a large volume of conductive fluid should vary with $\sqrt{d}$ (see Jack, Noble & Tsien, 1975, for discussion concerning this relation in nerve fibres). However, contrary to this prediction, θ was found to be independent of diameter in both cultured strands of chick ventricle and sheep Purkinje fibres (Lieberman, Kootsey, Johnson & Sawanobori, 1973; Schoenberg *et al.* 1975). The existence of anisotropy within the Purkinje fibre (with transverse resistance much greater than longitudinal resistance) would explain this result because the active currents at the edge of the propagating wave-front would flow preferentially within the column of cells wherein the impulse originated. Thus, conduction velocity would be independent of diameter provided the size of the fibres was determined by the number of cells contained rather than the size of the individual

cells. This circumstance (i.e. θ not dependent on d) might render advantages to the co-ordination of ventricular muscle contraction. The timing and hence co-ordination of Purkinje fibre impulses to the ventricles would be simplified if only the length and electrical characteristics of the conductive path were important and not the diameter of the fibres and their various branches.

A second observation into which anisotropy lends insight concerns the initiation of the propagated impulse and the liminal length for excitation (x_{LL}). Fozzard & Schoenberg (1972) described a much smaller ratio of x_{LL} to d.c. space constant ($x_{LL} \cong 0{\cdot}1$–$0{\cdot}2\ \lambda$) in cardiac Purkinje fibres than in point-stimulated squid axons ($x_{LL} \cong 0{\cdot}5$–$0{\cdot}55\ \lambda$). Noble (1972) attempted to explain this difference by approximating the current–voltage (I–V) relation above and below the 'uniform' voltage threshold (V_B) by linear relations: $I = g_r V$ and $I = g_1 V$, respectively (where g_r and g_1 are the resting and active membrane conductances). Noble's (1972) subsequent analysis led to a simple analytical expression for the normalized liminal length X_{LL}: $X_{LL} = (\pi/2)\lambda_B/\lambda = (\pi/2)\sqrt{(-g_r/g_1)}$ (where λ_B = space constant at V_B and λ = resting d.c. space constant). However, as pointed out by Schoenberg *et al.* (1975), such an analysis neglects the different geometries of the two structures. Excitation of a segment of squid axon involves charge movements within a core that is more-or-less equally accessible to the flow of charge. This is unlikely to be the case for point stimulation of the cardiac Purkinje fibre. In fact, the above considerations regarding the voltage distribution near the current source suggest that current flow and hence charge redistribution may be constrained within the excited region (with an effectively greater internal resistance near the current source than measured from longitudinal current flows some distance away). This would tend to concentrate depolarizing current near the current electrode, limit the influx of passive repolarizing currents, and thus promote the occurrence of excitation within a shorter segment (Schoenberg *et al.* 1975). Consequently, the shorter liminal length for the cardiac Purkinje fibre may be secondary (at least in part) to restriction of charge movements within the fibre interior.

In conclusion, the chief difference in one-dimensional cable properties between resting and active Purkinje fibres appears to be a voltage-dependent alteration in membrane resistance. Electrotonic potentials recorded close to a point-source of current deviate from the theoretical three-dimensional voltage distribution because of anisotropy. The existence of anisotropy may explain the independence of conduction velocity and fibre diameter. Furthermore, anisotropy constrains the flow of charge within the fibre leading to excitation over a smaller area than otherwise would be predicted.

The author would like to express his deep gratitude to Professor S. Weidmann and Dr R. Weingart for their encouragement and constructive criticism during this work. I also wish to thank Mr C. Cigada and Miss M. Herrenschwand for technical assistance. The author also gratefully acknowledges Miss H. Claassen for her assistance with the anatomical studies. The investigation was supported in part by grant HL06242 from the National Heart, Lung and Blood Institute, National Institutes of Health, Bethesda, MD, U.S.A.

REFERENCES

ADRIAN, R. H., COSTANTIN, L. L. & PEACHEY, L. D. (1969). Radial spread of contraction in frog muscle fibres. *J. Physiol.* **204**, 231–257.

BOYETT, M. R. & JEWELL, B. R. (1980). Analysis of the effects of changes in rate and rhythm upon electrical activity in the heart. *Prog. Biophys. & molec. Biol.* **36**, 1–52.

BREDIKIS, J., BUKAUSKAS, F. & VETEIKIS, R. (1981). Decreased intercellular coupling after prolonged rapid stimulation in rabbit atrial muscle. *Circulation Res.* **49**, 815–820.

CARMELIET, E. E. (1961). Chloride ions and the membrane potential of Purkinje fibres. *J. Physiol.* **156**, 375–388.

CLERC, L. (1976). Directional differences of impulse spread in trabecular muscle from mammalian heart. *J. Physiol.* **255**, 335–346.

COHEN, C. J., FOZZARD, H. A. & SHEU, S.-S. (1982). Increase in intracellular sodium ion activity during stimulation in mammalian cardiac muscle. *Circulation Res.* **50**, 651–662.

COHEN, I., FALK, R. & KLINE, R. (1981). Membrane currents following activity in canine cardiac Purkinje fibers. *Biophys. J.* **33**, 281–288.

EISENBERG, R. S. & JOHNSON, E. A. (1970). Three-dimensional electrical field problems in physiology. *Prog. Biophys. & molec. Biol.* **20**, 1–65.

FATT, P. & KATZ, B. (1953). The electrical properties of crustacean muscle fibres. *J. Physiol.* **120**, 171–204.

FOZZARD, H. A. (1966). Membrane capacity of the cardiac Purkinje fibre. *J. Physiol.* **182**, 255–267.

FOZZARD, H. A. & SCHOENBERG, M. (1972). Strength–duration curves in cardiac Purkinje fibres: effects of liminal length and charge distribution. *J. Physiol.* **226**, 593–618.

HALL, A. E., HUTTER, O. F. & NOBLE, D. (1963). Current–voltage relations of Purkinje fibres in sodium-deficient solutions. *J. Physiol.* **166**, 225–240.

HELLAM, D. C. & STUDT, J. W. (1974). Linear analysis of membrane conductance and capacitance in cardiac Purkinje fibres. *J. Physiol.* **243**, 661–694.

HODGKIN, A. L. (1954). A note on conduction velocity. *J. Physiol.* **125**, 221–224.

HODGKIN, A. L. & RUSHTON, W. A. H. (1946). The electrical constants of a crustacean nerve fibre. *Proc. R. Soc.* B **133**, 444–479.

JACK, J. J. B., NOBLE, D. & TSIEN, R. W. (1975). *Electric Current Flow in Excitable Cells.* Oxford: Clarendon Press.

KLINE, R. P., COHEN, I., FALK, R. & KUPERSMITH, J. (1980). Activity-dependent extracellular K^+ fluctuations in canine Purkinje fibres. *Nature, Lond.* **286**, 68–71.

KLINE, R. P. & MORAD, M. (1978). Potassium efflux in heart muscle during activity: extracellular accumulation and its implications. *J. Physiol.* **280**, 537–558.

KOOTSEY, J. M., JOHNSON, E. A. & LIEBERMAN, M. (1977). The cylindrical cell with a time-variant membrane resistance. Measuring passive parameters. *Biophys. J.* **17**, 145–154.

LADO, M. G., SHEU, S.-S. & FOZZARD, H. A. (1982). Changes in intracellular Ca^{2+} activity with stimulation in sheep cardiac Purkinje strands. *Am. J. Physiol.* **243**, H133–137.

LIEBERMAN, M., KOOTSEY, J. M., JOHNSON, E. A. & SAWANOBORI, T. (1973). Slow conduction in cardiac muscle. A biophysical model. *Biophys. J.* **13**, 37–55.

LIEBERMAN, M., SAWANOBORI, T., KOOTSEY, J. M. & JOHNSON, E. A. (1975). A synthetic strand of cardiac muscle. Its passive electrical properties. *J. gen. Physiol.* **65**, 527–550.

MOBLEY, B. A. & PAGE, E. (1972). The surface area of sheep cardiac Purkinje fibres. *J. Physiol.* **220**, 547–563.

NOBLE, D. (1972). The relation of Rushton's 'liminal length' for excitation to the resting and active conductances of excitable cells. *J. Physiol.* **226**, 573–591.

PRESSLER, M. L., ELHARRAR, V. & BAILEY, J. C. (1982). Effects of extracellular calcium ions, verapamil, and lanthanum on active and passive properties of canine cardiac Purkinje fibers. *Circulation Res.* **51**, 637–651.

SACHS, F. (1976). Electrophysiological properties of tissue cultured heart cells grown in a linear array. *J. Membrane Biol.* **28**, 373–399.

SCHOENBERG, M., DOMINGUEZ, G. & FOZZARD, H. A. (1975). Effect of diameter on membrane capacity and conductance of sheep cardiac Purkinje fibers. *J. gen. Physiol.* **65**, 441–458.

SNEDECOR, G. W. & COCHRAN, W. G. (1967). *Statistical Methods*, 6th edn. Ames, Iowa: The Iowa State University Press.

SPACH, M. S., KOOTSEY, J. M. & SLOAN, J. D. (1982). Active modulation of electrical coupling between cardiac cells of the dog. A mechanism for transient and steady state variations in conduction velocity. *Circulation Res.* **51**, 347–362.

VASSALLE, M. (1970). Electrogenic suppression of automaticity in sheep and dog Purkinje fibers. *Circulation Res.* **27**, 361–377.

WEIDMANN, S. (1952). The electrical constants of Purkinje fibres. *J. Physiol.* **118**, 348–360.

WEIDMANN, S. (1955). Rectifier properties of Purkinje fibers. *Am. J. Physiol.* **183**, 671.

WEIDMANN, S. (1970). Electrical constants of trabecular muscle from mammalian heart. *J. Physiol.* **210**, 1041–1054.